Molecules and Cells

MET1-Dependent DNA Methylation Represses Light Signaling and Influences Plant Regeneration in *Arabidopsis*

Sangrea Shim[1,2], Hong Gil Lee[2], and Pil Joon Seo[1,2,3,*]

[1]Department of Chemistry, Seoul National University, Seoul 08826, Korea, [2]Plant Genomics and Breeding Institute, Seoul National University, Seoul 08826, Korea, [3]Research Institute of Basic Sciences, Seoul National University, Seoul 08826, Korea
*Correspondence: pjseo1@snu.ac.kr
https://doi.org/10.14348/molcells.2021.0160
www.molcells.org

Plant somatic cells can be reprogrammed into a pluripotent cell mass, called callus, which can be subsequently used for *de novo* shoot regeneration through a two-step *in vitro* tissue culture method. MET1-dependent CG methylation has been implicated in plant regeneration in *Arabidopsis*, because the *met1-3* mutant exhibits increased shoot regeneration compared with the wild-type. To understand the role of MET1 in *de novo* shoot regeneration, we compared the genome-wide DNA methylomes and transcriptomes of wild-type and *met1-3* callus and leaf. The CG methylation patterns were largely unchanged during leaf-to-callus transition, suggesting that the altered regeneration phenotype of *met1-3* was caused by the constitutively hypomethylated genes, independent of the tissue type. In particular, MET1-dependent CG methylation was observed at the blue light receptor genes, *CRYPTOCHROME 1* (*CRY1*) and *CRY2*, which reduced their expression. Coexpression network analysis revealed that the *CRY1* gene was closely linked to cytokinin signaling genes. Consistently, functional enrichment analysis of differentially expressed genes in *met1-3* showed that gene ontology terms related to light and hormone signaling were overrepresented. Overall, our findings indicate that MET1-dependent repression of light and cytokinin signaling influences plant regeneration capacity and shoot identity establishment.

Keywords: *Arabidopsis*, callus, cryptochrome 1, cytokinin, DNA methylation, MET1, shoot regeneration

INTRODUCTION

Plant somatic cells can be reprogrammed to form an unorganized pluripotent cell mass, called callus. Incubation on callus-inducing medium (CIM) activates cell proliferation, facilitating callus formation. Accumulating evidence shows that callus tissue resembles root primordium, regardless of the origin of tissue explants (Atta et al., 2009; Sugimoto et al., 2010). Consistently, callus formation is initiated from pericycle-like cells (Sugimoto et al., 2010). The founder cell undergoes asymmetric cell division and then enables the acquisition of root primordium identity (Dubrovsky et al., 2000; Sugimoto et al., 2010), with the activation of genes including *WUSCHEL-RELATED HOMEOBOX 11* (*WOX11*) (Liu et al., 2014) and *LATERAL ORGAN BOUNDARIES DOMAINs* (*LBDs*) (Feng et al., 2012). Then, callus cells establish regeneration competence via the expression of root stem cell regulator genes, including *PLETHORA 1* (*PLT1*), *PLT2*, *SHORT-ROOT* (*SHR*), *SCARECROW* (*SCR*), and *WOX5* (Kareem et al., 2015; Sugimoto et al., 2010). After the acquisition of pluripotency, shoot regeneration can be triggered by incubating the callus on cytokinin-rich shoot-inducing medium (SIM). The cytoki-

Received 18 June, 2021; revised 2 August, 2021; accepted 24 August, 2021; published online 20 October, 2021

eISSN: 0219-1032

nin-inducible type-B ARABIDOPSIS RESPONSE REGULATOR (ARR)–WUSCHEL (WUS) module plays a crucial role in *de novo* shoot organogenesis from callus (Meng et al., 2017; Zhang et al., 2017). Shoot-specific physiological processes, including light signaling, also promote *de novo* shoot regeneration (Nameth et al., 2013).

Chemical modifications of DNA or core histone proteins alter chromatin structure, contributing to gene expression regulation, independent of the changes in DNA sequence. Methylation of the fifth carbon of cytosine residue is the most extensively studied epigenetic modification in both plants and mammals (Kim et al., 2021; Yoo et al., 2021). DNA methylation usually represses gene transcription (Chen et al., 2008; Jeddeloh et al., 1998; Zilberman et al., 2007), although increasing evidence shows that DNA methylation can also activate gene expression (Baubec et al., 2013; Brackertz et al., 2002; Fujita et al., 2003; Fukushige et al., 2006; Harris et al., 2018; Lang et al., 2017; Waterfield et al., 2014; Zemach and Grafi, 2003). The *Arabidopsis thaliana* genome is selectively methylated in CG, CHG, and CHH (H = A, T, or C) contexts. DOMAINS REARRANGED METHYLTRANSFERASE 2 (DRM2) catalyzes *de novo* methylation of cytosine residues in all sequence contexts (CG, CHG, and CHH) through the RNA-directed DNA methylation (RdDM) pathway (Cao and Jacobsen, 2002a). CG methylation is maintained by METHYLTRANSFERASE 1 (MET1) (Zubko et al., 2012), whereas the maintenance of CHG methylation requires CHROMOMETHYLASE 3 (CMT3) (Bartee et al., 2001; Lindroth et al., 2001). Maintenance of asymmetric CHH methylation is ensured by CMT2, DRM1, and DRM2 (Cao and Jacobsen, 2002b). In addition, cytosine methylation can be reversibly removed by the DNA glycosylase/lyase mechanism. In *Arabidopsis*, REPRESSOR OF SILENCING 1 (ROS1), DEMETER (DME), DME-LIKE 2 (DML2), and DML3 proteins facilitate DNA base excision repair (BER) as an active demethylation mechanism (Ortega-Galisteo et al., 2008; Penterman et al., 2007).

DNA methylation is closely associated with plant regeneration. For example, MET1-dependent DNA methylation negatively controls the expression of core shoot regeneration regulator genes, including *WUS*, and represses *de novo* shoot organogenesis on CIM (Li et al., 2011; Liu et al., 2018). The *met1* mutant displays enhanced *WUS* expression and thereby higher rates of shoot regeneration without incubation on CIM. Moreover, spatiotemporal expression of *MET1* is delicately regulated via the dual mode of action of cytokinin on SIM. At the early stage of shoot induction, *MET1* expression in calli is induced by the cytokinin–CYCD3–E2FA module, repressing *WUS* expression. With increasing incubation time on SIM, *MET1* expression is restricted to the outer cell layers of the callus, whereas *WUS* expression is activated by type-B ARRs in cell layers beneath the MET1-expressing regions (Liu et al., 2018).

In this study, we conducted whole-genome bisulfite sequencing (BS-seq) of the *met1-3* mutant and wild-type, and compared the changes in CG methylation landscape between the two genotypes during callus formation to understand the role of MET1 in plant regeneration. Notably, CG methylation was largely unchanged during leaf-to-callus transition, regardless of genotypes. Thus, the enhanced shoot regeneration phenotype of *met1-3* was caused by the constitutively hypomethylated genes. We particularly focused on MET1-dependent CG methylation at the blue light receptor loci, *CRYPTOCHROME 1* (*CRY1*) and *CRY2*. MET1-dependent CG methylation repressed the expression of both *CRY* genes. CRY1 subsequently regulated cytokinin signaling, especially type-B *ARR* genes. Given that shoot regeneration requires cytokinin signaling, enhanced cytokinin signaling possibly led to enhanced *de novo* shoot regeneration in *met1-3*. Overall, our results suggest that MET1-dependent CG methylation negatively regulates light and cytokinin signaling and influences plant regeneration.

MATERIALS AND METHODS

Plant materials and growth conditions

Arabidopsis met1-3 (Johnson et al., 2007), *cry1-1* (Koornneef et al., 1980), and *cry2/fha-1* (Koornneef et al., 1991) mutants have been described previously. Seeds were germinated on Murashige and Skoog (MS) medium at 22°C-23°C under a long-day photoperiod (16 h light/8 h dark) with fluorescent light (150 μmol photons/m^2s). The third and fourth leaves of two-week-old seedlings were used as explants to induce callus on CIM (B5 medium supplemented with 0.5 μg/ml 2,4-dichlorophenoxyacetic acid [2,4-D] and 0.05 μg/ml kinetin). The plates were incubated at 22°C under continuous dark for 2 weeks (Fan et al., 2012). To induce *de novo* shoot regeneration, leaf explant-derived callus preincubated on CIM for 7 days was transferred to SIM (B5 medium supplemented with 0.9 μmol/L indole-3-acetic acid and 2.5 μmol/L 2-isopentenyladenine). The plates were incubated at 25°C under continuous light for up to 3 weeks to examine the shoot regeneration capacity of the callus.

Whole genome BS-seq

BS-seq libraries were constructed as described previously (Shim et al., 2021). Callus samples are heterogeneous and exhibit significant variation in gene expression; therefore, a large amount of sample (>1 g) was used to perform high-depth BS-seq (>70× coverage) for single biological replicate. The third and fourth leaves of *in vitro*-cultured 2-week-old seedlings were used for immediately harvesting leaf explants and for inducing callus on CIM. Using the cetyltrimethylammonium bromide (CTAB) method, genomic DNA was extracted from leaf explants and leaf explant-derived calli incubated on CIM for 2 weeks. Then, 5 μg of each genomic DNA sample was fragmented by Covaris shearing (Covaris, USA). Blunt-ended and phosphorylated fragments were adenylated at the 3'-ends, and ligated to a methylated adapter using the TruSeq DNA Library Preparation Kit (Illumina, USA). Then, ligation products were separated by agarose gel electrophoresis, and 275-350 bp products were purified. The purified fragments were bisulfite-treated using the EpiTect Bisulfite Conversion Kit (Qiagen, Germany), according to the manufacturer's instructions. Bisulfite conversion was performed in a thermal cycler under the following conditions: (1) denaturation at 95°C for 5 min, (2) incubation at 60°C for 25 min, (3) denaturation at 95°C for 5 min, (4) incubation at 60°C for 85 min, (5) denaturation at 95°C for 5 min, (6) incubation at

60°C for 175 min, and (7) hold at 20°C. Bisulfite-converted DNA samples were purified twice using 20 μl of elution buffer included in the EpiTect kit. The bisulfite-treated fragments were amplified by polymerase chain reaction (PCR) using a primer cocktail included in the TruSeq kit to generate products with adaptors on both ends. The final products were used for constructing a BS-seq library, which was sequenced on the HiSeq2000 platform (Illumina).

BS-seq data analysis and differentially methylated region (DMR) identification

Raw BS-seq reads were analyzed as described previously (Smallwood et al., 2014), with slight modifications. Briefly, according to the Bismark Bisulfite Mapper guidelines (https://rawgit.com/FelixKrueger/Bismark/master/Docs/Bismark_User_Guide.html), the first 8 bp of raw BS-seq reads were trimmed using TrimGalore (parameters: --gzip --paired --clip_R1 8 --clip_R2 8) to prevent adaptor contamination (Krueger and Andrews, 2011). The trimmed reads were initially aligned to the TAIR10 version of the *Arabidopsis* reference genome sequence (https://www.arabidopsis.org/) using Bismark (Krueger and Andrews, 2011) and Bowtie2 (Langmead and Salzberg, 2012), with default parameters, according to the guideline of Bismark Bisulfite Mapper. Then, PCR duplicates in initial alignment files were purged using the deduplicate_bismark script. Bisulfite treatment was validated by calculating the fraction of unmethylated cytosine residues (C to T conversion rate > 99.0%) among the total number of mapped cytosines in the chloroplast genome. The average bisulfite conversion rate was greater than 98.4%, indicating successful bisulfite treatment. The mapped read statistics are summarized in Supplementary Table S1. Considering the cumulative number of cytosines in all examined samples, individual methyl-cytosines with more than five supporting reads were selected for further analysis (Supplementary Fig. S1).

To identify DMRs between *met1-3* and wild-type genotypes, the Bismark output files were converted into bedGraph format using the bismark2bedGraph script, with –CX and –zero_based options. The output bedGraph files of *met1-3* and wild-type leaf and callus samples were used as input for DMRfinder (Gaspar and Hart, 2017), and methylated regions for each methylation context were defined using the following criteria: maximum methylated region length, 500 bp; minimum number of methylcytosines, 3; maximum distance between methylcytosines, 100 bp; and minimum total read count > 20. Regions with significant difference in methylation levels ($P < 0.05$), i.e., more than 40%, 20%, and 10% absolute difference in the methylation of CG, CHG, and CHH contexts, respectively, between *met1-3* and wild-type (for both leaf and callus tissues) were identified as DMRs, as reported previously (Bhatia et al., 2018; Chen et al., 2018; Liang et al., 2019; Liu et al., 2016; Stassen et al., 2018; Zhou et al., 2019).

To determine whether DMRs overlapped with genic regions (defined as the region encompassing the gene body and 1 kb sequence upstream of the transcription start site) and transposable element (TE) regions, the BS-seq data were investigated using BEDTools (Quinlan and Hall, 2010), based on the TAIR10 reference genome annotation. Genome-wide patterns of DNA methylation were visualized using Pandas, NumPy, SciPy, and pyplot libraries of Python. The cytosine conversion rate in genic regions was depicted using deepTools (Ramírez et al., 2014).

Functional enrichment and coexpression network analyses

To analyze the enriched biological functions of differentially methylated genes, the MapMan annotation was used for comparing the observed ratio of genes of interest (GOIs) in a selected gene group with the expected ratio of genes in the reference genome for a specific pathway through the hypergeometric test using a homemade Python script (Usadel et al., 2009). Moreover, to construct a coexpression network, the GOIs were inputted as queries into the NetworkDrawer implemented in ATTED-II (https://atted.jp) (Obayashi et al., 2018).

RNA-seq analysis

To analyze the impact of DNA methylation on gene expression in the wild-type and *met1-3* mutant, the RNA-seq data of wild-type leaf explants generated previously (Lee et al., 2016) were used in this study. Additionally, high-depth RNA-seq analysis of *met1-3* was performed in the current study using a large amount of leaf explants (>1 g) for single biological replicate.

Quantitative real-time reverse transcription PCR (RT-qPCR) analysis

Total RNA was extracted from *met1-3* and wild-type leaf explants and callus tissues using the TRI reagent (TAKARA Bio, Japan), according to the manufacturer's recommendations, and treated with an RNase-free DNase to eliminate genomic DNA contamination. The first-strand cDNA was synthesized from 2 μg of total RNA by reverse transcription using Moloney Murine Leukemia Virus reverse transcriptase (Dr. Protein, Korea) with oligo(dT18) primers. RT-qPCR experiments were performed on the Step-One Plus Real-Time PCR System (Applied Biosystems, USA). The comparative C_T method was used to determine relative gene expression using the *EUKARYOTIC TRANSLATION INITIATION FACTOR 4A1* (*eIF4A*) gene (At3g13920) as an internal control. All RT-qPCR reactions were performed using three independent replicate samples. The specificity of RT-qPCR results was determined by melt curve analysis of the amplified products using the standard method.

Data availability

Whole genome BS-seq and RNA-seq data are available at the National Center for Biotechnology Information (NCBI) Sequence Read Archive (SRA) data under the BioProject accession number PRJNA601842.

RESULTS

Enhanced shoot regeneration in *met1-3*

MET1 is involved in plant regeneration from root and pistil tissues (Li et al., 2011; Liu et al., 2018). To further analyze the functional impact of MET1 in plant regeneration, we performed the two-step *in vitro* plant regeneration process

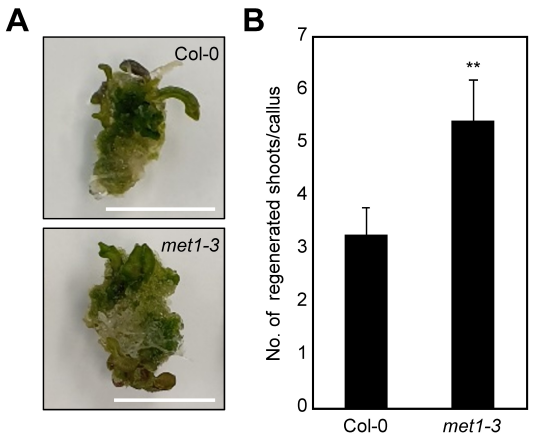

Fig. 1. Increased *de novo* shoot regeneration efficiency in the *met1-3* mutant. (A) Shoot regeneration phenotypes. (B) Number of regenerated shoots. In (A) and (B), calli preincubated for 7 days on CIM were transferred to SIM. The number of regenerated shoots from calli was measured ($n > 30$) at 3 weeks after incubation on SIM. Error bars indicate the SEM. Statistically significant differences between wild-type and mutant calli are indicated by asterisks (Student's *t*-test, $**P < 0.01$). Scale bars = 10 mm.

using leaf explants. The third and fourth leaves of 2-week-old seedlings were excised and placed on CIM. Upon callus emergence, callus tissues were transferred to SIM in order to induce shoot regeneration.

Plant regeneration capacity was determined by monitoring *de novo* shoot organogenesis from calli on SIM. The *met1-3* mutant calli displayed greater shoot regeneration than wild-type calli (Fig. 1). These results suggest that MET1 possibly regulates *de novo* shoot organogenesis-related processes and affects plant regeneration.

Global changes in DNA methylation in *met1-3*

To understand the molecular basis of enhanced *de novo* shoot regeneration in *met1-3*, we conducted whole-genome BS-seq using *met1-3* and wild-type leaf explants and leaf explant-derived calli (Fig. 2A, Supplementary Table S1, Supplementary Fig. S1). Because MET1 plays a major role in maintaining CG methylation in *Arabidopsis* (Zubko et al., 2012), we particularly focused on CG methylation in this study. The BS-seq results showed that CG methylation was extensively diminished in *met1-3*, regardless of the tissue type (Fig. 2B), whereas global CHG and CHH methylation levels were rather increased in *met1-3* compared with the wild-

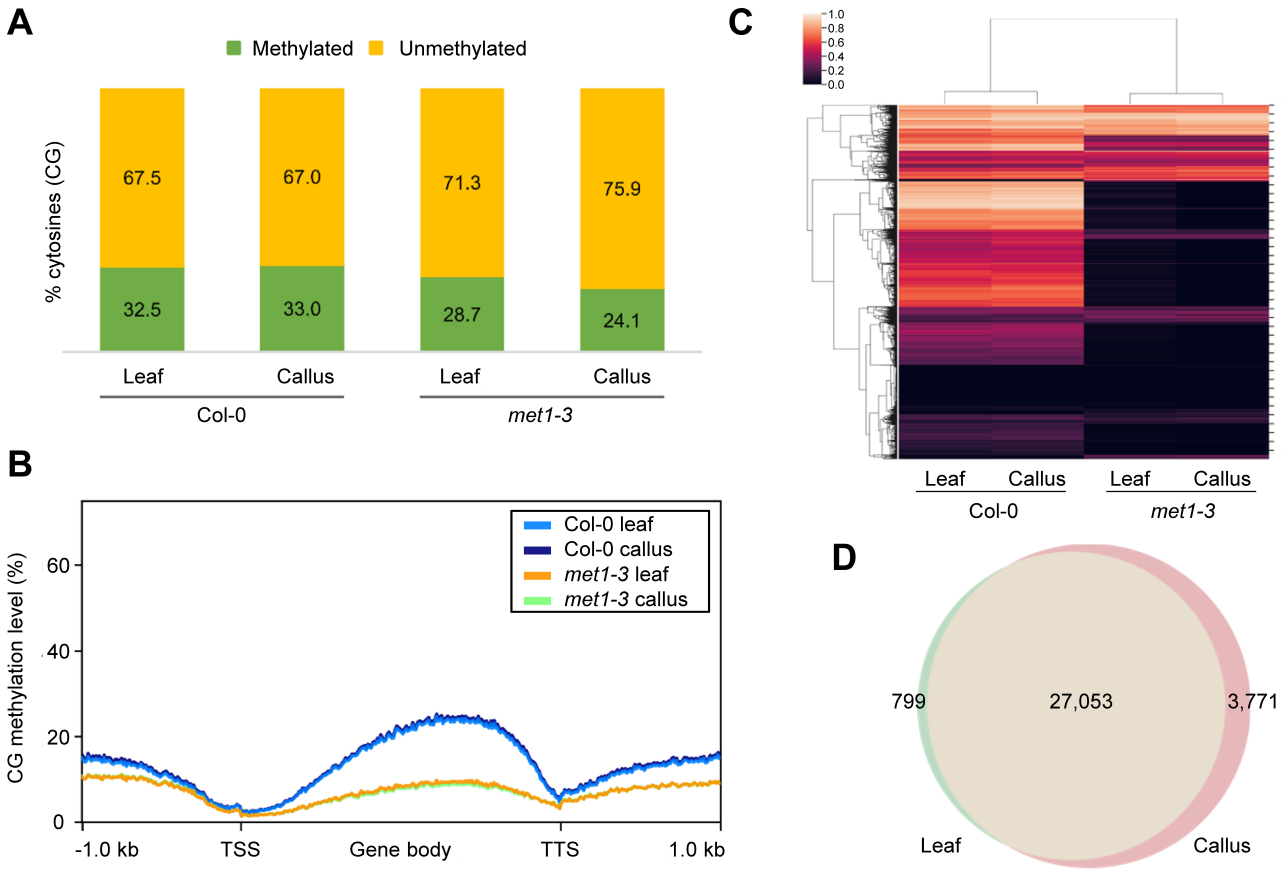

Fig. 2. Marginal changes in CG methylation during leaf-to-callus transition. (A) Fractions of methylated and unmethylated cytosines in the CG context in wild-type and *met1-3*. (B) Average CG methylation levels over genic regions in wild-type and *met1-3*. TSS, transcription start site; TTS, transcription termination site. (C) Hierarchical clustering of genome-wide CG methylation patterns. The color bar indicates the methylation level. (D) Venn diagram of regions hypomethylated in each tissue of *met1-3* relative to that of the wild-type.

type (Supplementary Fig. S2). Most DMRs in *met1-3* were also concentrated in the CG context (Supplementary Fig. S2). Furthermore, during leaf-to-callus transition, CHG and CHH methylation was significantly changed particularly at TE regions in wild type (Supplementary Fig. S2B), consistent with a previous study showing that dynamic changes in CHG and CHH methylation levels in TE regions affect plant regeneration (Shim et al., 2021). However, the changes observed in CHG and CHH methylation levels during callus formation were maintained in *met1-3* mutant (Supplementary Fig. S2), suggesting that the role of MET1 in plant regeneration is related primarily to CG methylation, independent of CHG and CHH methylation.

Notably, the CG methylation level showed a negligible change during leaf-to-callus transition both in the wild-type and *met1-3* mutant (Fig. 2B). Hierarchical clustering analysis also showed that CG methylation patterns for the same genotype were similar in both calli and leaves (Fig. 2C), consistent with the minor changes in CG methylation observed previously during plant growth and development (Ingouff et al., 2017; Ito et al., 2019; Saze et al., 2003). Because CG methylation levels were mostly reduced in *met1-3* (Fig. 2C), we collected CG regions hypomethylated in *met1-3* relative to the wild-type. The results showed that 27,852 and 30,824 genomic regions were hypomethylated in leaf (Supplementary Table S2) and callus (Supplementary Table S3) tissues, respectively, in *met1-3*. Notably, most of these regions (27,053) were commonly hypomethylated in both leaf (97.1%; 27,053 of 27,852) and callus (87.8%; 27,053 of 30,824) tissues (Fig. 2D), indicating that CG methylation is not dynamically reprogrammed during the course of callus formation.

Given that most of the hypomethylated CG-DMRs were found in genic regions (Supplementary Fig. S2), we collected genes containing hypomethylated CG regions in *met1-3* within genic regions (Supplementary Tables S4 and S5). GO enrichment analysis revealed that MET1-dependent CG methylation regulates a variety of biological processes, and most of these processes were commonly enriched in both leaf and callus tissues (Supplementary Tables S6-S8). In particular, hypomethylated genes in *met1-3* were enriched for GO terms related to light signaling (external stimuli response for red/far-red light [*P* value = 1.27×10^{-2} and 2.26×10^{-2} for leaf and callus tissues, respectively]) (Supplementary Table S6). Overall, these results suggest that the increased shoot regeneration efficiency of the *met1-3* mutant is attributable to its constitutively hypomethylated regions, which are possibly associated with light signaling.

MET1-mediated CG methylation at the *CRY1* and *CRY2* loci

To further understand the biological processes regulated by MET1, we conducted RNA-seq analysis and identified genes differentially expressed between *met1-3* and the wild-type. Because CG methylation levels did not change during callus formation in both genotypes, we used only leaf tissues to examine which genes were misregulated in *met1-3* prior to callus formation. A total of 3,935 differentially expressed genes (DEGs) were identified. Among these, 1,769 genes were up-regulated and 2,166 genes were down-regulated in the *met1-3* mutant compared with the wild-type (Supplementary Table S9).

GO enrichment analysis of the DEGs showed that GO terms related to light signaling and responses were significantly enriched for light signaling and responses (external stimuli response for UV-A/blue light [*P* value = 7.46×10^{-3}] and UV-B light [*P* value = 2.41×10^{-2}]) (Table 1), which is consistent with the fact that MET1-dependent CG-DMRs were enriched in genes involved in light signaling (Supplementary Table S6). In addition, it was notable that auxin (phytohormone action for auxin biosynthesis [*P* value = 1.41×10^{-2}]) and cytokinin-related processes (phytohormone action for cytokinin perception and signal transduction [*P* value = 9.61×10^{-3}] and cytokinin transport [*P* value = 2.09×10^{-2}]) were also overrepresented (Table 1). These results suggest that DNA methylation-dependent regulation of light signaling ultimately affects hormone signaling, which may account for the altered plant regeneration phenotype of the *met1-3* mutant (Fig. 1).

The biological impact of light signaling on plant regeneration remains unknown; therefore, we decided to investigate how light signaling regulates *de novo* shoot regeneration. We revisited the hypomethylated regions in *met1-3*, and found that key blue light receptor genes, including *CRY1* and *CRY2*, were under the control of MET1-dependent CG methylation (Fig. 3A) in both leaf and callus tissues (Supplementary Tables S4 and S5). Expression levels of *CRY1* and *CRY2* were higher in *met1-3* than in the wild-type (Fig. 3A, Supplementary Table S10), suggesting that CG methylation repressed the expression of these genes. To validate the transcriptional control over photoreceptor genes by MET1, we carried out RT-qPCR analysis using *met1-3* and wild-type calli. The expression of *CRY* genes gradually decreased in the wild-type during callus formation, but the reduction was diminished in *met1-3* (Fig. 3B, Supplementary Fig. S3), indicating that light signaling triggered by *CRY1* and *CRY2* is derepressed in *met1-3*. The contradicting results of *CRY* expression in leaf tissues between RNA-seq and RT-qPCR might be explained by the differential sensitivity of the two techniques.

Next, we investigated whether shoot regeneration efficiency of *met1-3* was indeed associated with increased expression of *CRY*s. To test this possibility, we employed *cry1-1* and *cry2/fha-1* mutants, and examined their *de novo* shoot regeneration capacity. The *cry1-1* mutant particularly displayed reduced shoot regeneration (Figs. 3C and 3D), while *cry2/fha-1* showed a statistically insignificant increase in shoot regeneration efficiency (Supplementary Fig. S3), compared with wild type. Given that CRY1 is responsible for sensing both low and high intensities of blue light, whereas CRY2 mainly perceives a low intensity of blue light (Lin et al., 1998; Yu et al., 2010), it is reasonable to speculate that CRY1 has a broad and greater impact during plant regeneration. Together, these data suggest that MET1-dependent CG methylation represses *CRY1* expression and influences the plant regeneration process.

Coexpression of *CRY1* and cytokinin signaling genes

To estimate the extent of the biological impact of MET1

Table 1. Functional enrichment analysis of DEGs in *met1-3* relative to the wild-type

Functional category[a]	No. of query genes per category	Total No. of query genes	Observed value (%)	No. of reference genes per category	Total No. of reference genes	Expected value (%)	*P* value
RNA biosynthesis (transcriptional regulation)	442	3,936	11.2	1,962	27,206	7.2	1.87E-23
Enzyme classification (EC_2 transferases)	100	3,936	2.5	382	27,206	1.4	1.22E-09
Enzyme classification (EC_1 oxidoreductases)	87	3,936	2.2	420	27,206	1.5	2.94E-04
Solute transport (carrier-mediated transport)	148	3,936	3.8	784	27,206	2.9	3.42E-04
External stimuli response (pathogen)	53	3,936	1.3	233	27,206	0.9	4.55E-04
Vesicle trafficking (clathrin-independent machinery)	3	3,936	0.1	3	27,206	0.0	3.03E-03
Carbohydrate metabolism (fermentation)	4	3,936	0.1	6	27,206	0.0	5.14E-03
Carbohydrate metabolism (oligosaccharide metabolism)	6	3,936	0.2	13	27,206	0.0	6.27E-03
Phytohormone action (ethylene-biosynthesis)	7	3,936	0.2	17	27,206	0.1	6.75E-03
External stimuli response (light-UV-A/blue light)	10	3,936	0.3	30	27,206	0.1	7.46E-03
Protein modification (phosphorylation)	195	3,936	5.0	1,148	27,206	4.2	8.34E-03
Lipid metabolism (lipid bodies-associated activities)	12	3,936	0.3	40	27,206	0.1	8.99E-03
Cell wall organization (pectin)	39	3,936	1.0	185	27,206	0.7	9.17E-03
Phytohormone action (cytokinin-perception and signal transduction)	10	3,936	0.3	31	27,206	0.1	9.61E-03
Protein modification (S-glutathionylation)	19	3,936	0.5	76	27,206	0.3	1.06E-02
Phytohormone action (abscisic acid-conjugation and degradation)	5	3,936	0.1	11	27,206	0.0	1.36E-02
Phytohormone action (auxin-biosynthesis)	6	3,936	0.2	15	27,206	0.1	1.41E-02
External stimuli response (gravity)	6	3,936	0.2	15	27,206	0.1	1.41E-02
Multi-process regulation (programmed cell death [PCD] system)	9	3,936	0.2	29	27,206	0.1	1.79E-02
DNA damage response (photoreactivation)	2	3,936	0.1	2	27,206	0.0	2.09E-02
Phytohormone action (cytokinin-transport)	2	3,936	0.1	2	27,206	0.0	2.09E-02
Phytohormone action (signaling peptides)	43	3,936	1.1	219	27,206	0.8	2.16E-02
Phytohormone action (abscisic acid-transport)	3	3,936	0.1	5	27,206	0.0	2.41E-02
External stimuli response (light-UV-B light)	3	3,936	0.1	5	27,206	0.0	2.41E-02
Solute transport (channels)	35	3,936	0.9	180	27,206	0.7	4.00E-02
Phytohormone action (gibberellin-biosynthesis)	5	3,936	0.1	14	27,206	0.1	4.07E-02
Multi-process regulation (phosphatidylethanolamine-binding [PEB] protein-dependent signaling)	3	3,936	0.1	6	27,206	0.0	4.30E-02
Phytohormone action (salicylic acid-conjugation and degradation)	3	3,936	0.1	6	27,206	0.0	4.30E-02
Phytohormone action (gibberellin-perception and signal transduction)	4	3,936	0.1	10	27,206	0.0	4.44E-02
Multi-process regulation (SnRK1-kinase regulatory system)	8	3,936	0.2	29	27,206	0.1	4.88E-02

[a]Significantly overrepresented terms ($P < 0.05$) are presented. Statistical significance was determined by the hypergeometric test.

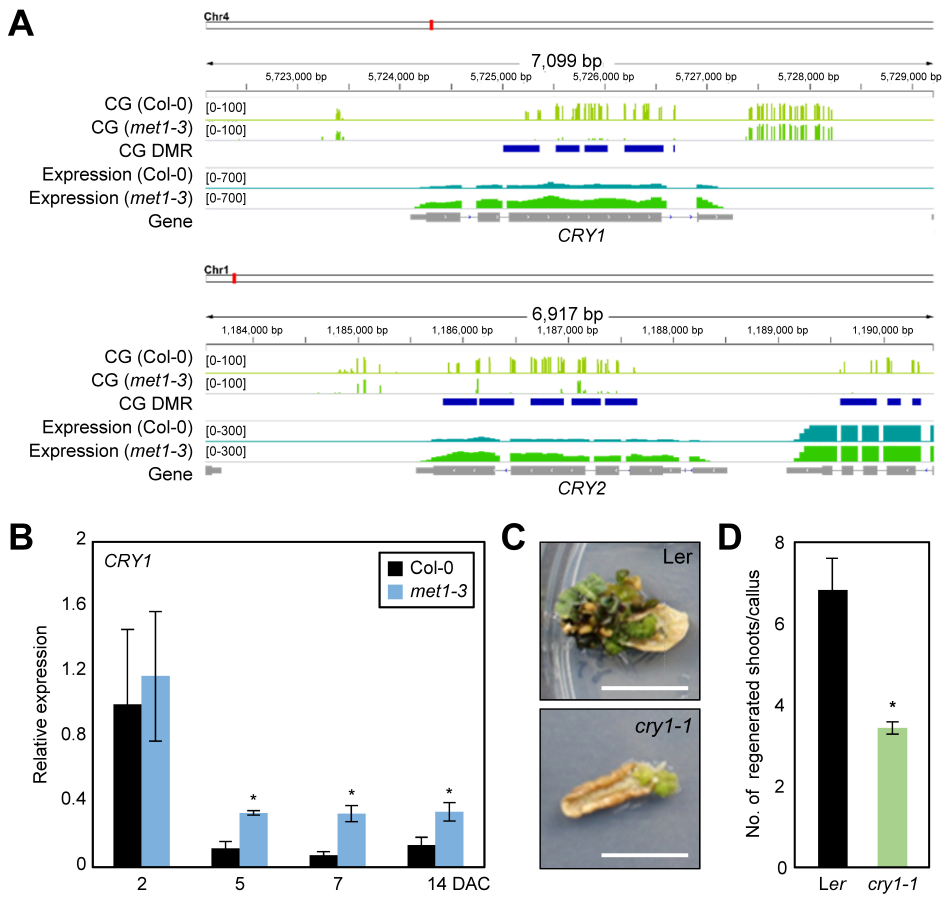

Fig. 3. MET1-dependent CG methylation at the *CRY* loci. (A) CG methylation patterns at the chromatin of *CRY1* and *CRY2* genes. DNA methylation states and mRNA levels are depicted. (B) Transcript level of *CRY1* in *met1-3* determined by RT-qPCR. Three independent biological replicates were averaged. Asterisks indicate significant differences (Student's *t*-test; $*P < 0.05$). DAC, days after incubation on CIM. (C and D) Shoot regeneration capacity of the *cry1-1* mutant. Calli preincubated for 7 days on CIM were transferred to SIM. The number of regenerated shoots from calli was measured (n > 30) at 3 weeks after incubation on SIM. Statistically significant differences between wild-type and mutant calli are indicated by asterisks (Student's *t*-test, $*P < 0.05$). Scale bars = 10 mm.

during plant regeneration, we identified genes both hypomethylated and up-regulated in *met1-3* (Supplementary Table S10); these genes included *CRY1* and *CRY2*. A total of 386 genes were identified, which were then subjected to coexpression network analysis. Of the 386 genes, 314 were included in a scaled-subnetwork consisting of 3,390 genes (Fig. 4A, Supplementary Table S11). To characterize the network, we performed functional enrichment analysis of all 3,390 genes. The results showed that cytokinin signaling was particularly overrepresented (phytohormone action for cytokinin-perception and signal transduction [*P* value = 3.95×10^{-5}]) (Table 2). Consistently, core cytokinin signaling genes, such as *ARR1* and *ARR9*, were found in the coexpression network (Fig. 4A).

In agreement with the finding that blue light receptor genes were included in the coexpression network of genes regulated by MET1-dependent CG methylation (Fig. 4A), the *CRY1* gene was also closely connected to cytokinin signaling. Gene regulatory network analysis showed that type-A and type-B *ARR* genes were particularly coexpressed with *CRY1* in a relation of second neighbor (Fig. 4B). Given that photoreceptors are involved in shoot identity establishment (Ikeuchi et al., 2016; Nameth et al., 2013), which requires cytokinin biosynthesis and signaling (Meng et al., 2017; Skoog and Miller, 1957; Zhang et al., 2017), it is plausible that *CRY1* is functionally associated with cytokinin signaling.

Considering that enhanced cytokinin signaling promotes *de novo* shoot organogenesis (Atta et al., 2009; Skoog and Miller, 1957; Sugimoto et al., 2010), the functions of MET1 and CRY1 in shoot regeneration were likely owing to altered cytokinin signaling. To test this possibility, we examined whether the transcript levels of cytokinin signaling genes were affected in *met1-3* and *cry1-1* mutants. Type-B *ARR1* and *ARR10* genes were up-regulated in *met1-3* (Fig. 4C) but were significantly repressed in *cry1-1* (Fig. 4D), as expected. These results indicate that MET1-dependent CG methylation represses *CRY1* and consequently cytokinin signaling, thus affecting plant regeneration.

Taken together, our findings demonstrate that MET1-dependent CG methylation represses *CRY1* expression and consequently reduces cytokinin signaling. In the *met1-3* mutant, methylation-free contexts at the *CRY1* locus activate gene expression and enhance cytokinin signaling (Fig. 5). The signaling axis encompassing MET1 and CRY1 influences the plant regeneration process, which is intrinsically based on the balance between auxin and cytokinin signaling.

DISCUSSION

In vitro plant regeneration involves two steps: callus formation and *de novo* shoot regeneration. Callus tissue is analogous to the lateral root primordium (Sugimoto et al., 2010); therefore, callus formation is initiated by genes involved in lateral root formation, including *LBDs*. Callus cells then estab-

Table 2. Functional enrichment analysis of all genes contained in the coexpression subnetwork shown in Fig.4A

Functional category[a]	No. of query genes per category	Total No. of query genes	Observed value (%)	No. of reference genes per category	Total No. of reference genes	Expected value (%)	*P* value
External stimuli response (pathogen)	66	3,391	1.9	233	27,206	0.9	6.60E-11
Nutrient uptake (iron uptake)	26	3,391	0.8	61	27,206	0.2	4.10E-09
Protein modification (phosphorylation)	207	3,391	6.1	1,148	27,206	4.2	1.85E-08
Enzyme classification (EC_2 transferases)	80	3,391	2.4	382	27,206	1.4	1.88E-06
Carbohydrate metabolism (starch metabolism)	19	3,391	0.6	52	27,206	0.2	7.85E-06
Phytohormone action (cytokinin-perception and signal transduction)	13	3,391	0.4	31	27,206	0.1	3.95E-05
Amino acid metabolism (degradation)	19	3,391	0.6	58	27,206	0.2	4.64E-05
Protein homeostasis (autophagy)	17	3,391	0.5	50	27,206	0.2	6.78E-05
Protein modification (S-glutathionylation)	20	3,391	0.6	76	27,206	0.3	8.02E-04
Cytoskeleton organization (microtubular network)	29	3,391	0.9	132	27,206	0.5	1.56E-03
Nutrient uptake (copper uptake)	9	3,391	0.3	24	27,206	0.1	1.61E-03
Phytohormone action (jasmonic acid-biosynthesis)	8	3,391	0.2	21	27,206	0.1	2.61E-03
Cell cycle organization (cytokinesis)	18	3,391	0.5	74	27,206	0.3	3.66E-03
Phytohormone action (salicylic acid-perception and signal transduction)	3	3,391	0.1	4	27,206	0.0	7.02E-03
Solute transport (channels)	34	3,391	1.0	180	27,206	0.7	8.53E-03
Solute transport (carrier-mediated transport)	120	3,391	3.5	784	27,206	2.9	9.78E-03
Multi-process regulation (target of rapamycin [TOR] signaling)	5	3,391	0.1	12	27,206	0.0	1.11E-02
Phytohormone action (salicylic acid-biosynthesis)	2	3,391	0.1	2	27,206	0.0	1.55E-02
Nutrient uptake (sulfur assimilation)	5	3,391	0.1	13	27,206	0.0	1.63E-02
Enzyme classification (EC_1 oxidoreductases)	67	3,391	2.0	420	27,206	1.5	2.01E-02
Cell cycle organization (DNA replication)	16	3,391	0.5	76	27,206	0.3	2.36E-02
Vesicle trafficking (target membrane tethering)	17	3,391	0.5	84	27,206	0.3	2.87E-02
Phytohormone action (salicylic acid-conjugation and degradation)	3	3,391	0.1	6	27,206	0.0	2.89E-02
Enzyme classification (EC_3 hydrolases)	41	3,391	1.2	251	27,206	0.9	4.22E-02
Vesicle trafficking (clathrin-independent machinery)	2	3,391	0.1	3	27,206	0.0	4.27E-02
Chromatin organization (chromatin remodeling complexes)	13	3,391	0.4	63	27,206	0.2	4.48E-02

[a]Significantly overrepresented terms ($P < 0.05$) were shown. Statistical significance was determined by the hypergeometric test.

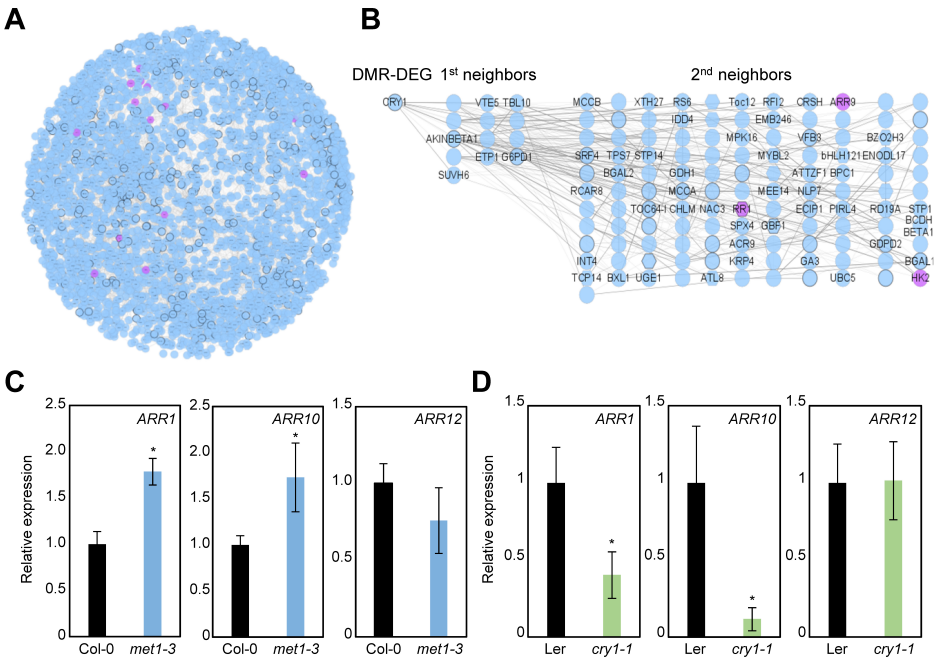

Fig. 4. Potential connection of *CRY1* and cytokinin signaling components. (A) Coexpression network of genes hypomethylated and up-regulated in *met1-3*. Cytokinin signaling genes are indicated by purple nodes. (B) Close neighbor genes of *CRY1* in the coexpression subnetwork. Cytokinin signaling genes are indicated by purple nodes. (C and D) Transcript levels of type-B *ARR* genes in *met1-3* (C) and *cry1-1* (D) calli determined by RT-qPCR. Three independent biological replicates were averaged. Asterisks indicate significant differences (Student's *t*-test; $*P < 0.05$).

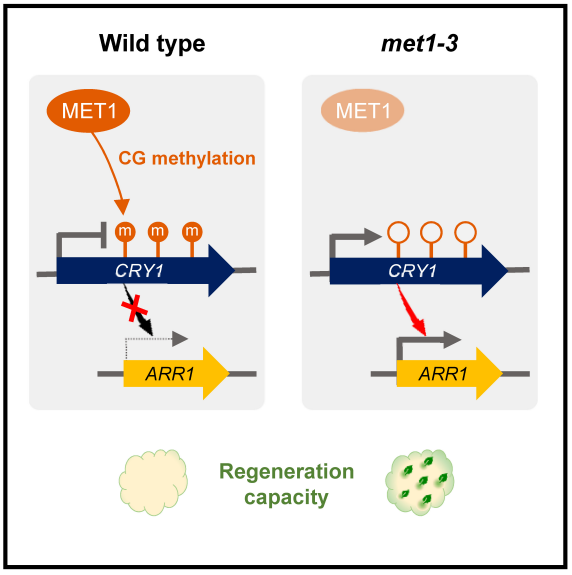

Fig. 5. The role of MET1 in *de novo* shoot regeneration. The *CRY1* gene is silenced by MET1-dependent DNA methylation to ensure homeostasis of light signaling in wild-type leaves. In *met1-3*, the CG methylation-free *CRY1* locus is transcriptionally activated, which stimulates the expression of cytokinin signaling genes, such as type-B *ARR*s. Increased cytokinin signaling promotes *de novo* shoot regeneration.

lish the root stem cell niche through the expression of pluripotency regulators, *PLT*s and *WOX*s (Kareem et al., 2015; Sugimoto et al., 2010). PLT- and WOX-induced root stem cell identity is considered as the cellular nature of pluripotency (Gaillochet and Lohmann, 2015; Lee and Seo, 2018), facilitating consequent tissue regeneration. After pluripotency acquisition, *de novo* shoot organogenesis can be initiated on SIM through the activation of type-B *ARR*s (Meng et al., 2017) and subsequently *WUS*, which defines the shoot developmental program (Zhang et al., 2017).

Plant regeneration involves substantial changes in the epigenetic landscape. Histone H3 modifications, including trimethylation of lysine 4 and lysine 36 residues (H3K4me3 and H3K36me3, respectively) and acetylation, exhibit dynamic changes during leaf-to-callus transition (Kim et al., 2018; Lee et al., 2017; Li et al., 2011). Various chromatin modifiers and remodelers have been identified as key regulators of cell fate transition (He et al., 2012; Ishihara et al., 2019). DNA methylation is also altered during the process of plant regeneration. In particular, genome-wide CHG and CHH methylation levels change during callus formation (Shim et al., 2021). By contrast, in this study, CG methylation was largely insensitive to cell fate transition, and CG methylation landscapes were mostly maintained during leaf-to-callus transition. It is plausible that CG methylation evolved to ensure genome integrity rather than to regulate gene expression.

Given the stable nature of CG methylation during leaf-to-callus transition, the altered *de novo* shoot regeneration capacity of *met1-3* was attributable to its constitutively hypomethylated genomic regions, independent of the tissue type. It has been demonstrated that the *WUS* gene, a key regulator of shoot stem cell formation, is constitutively activated in *met1*, which accounts for their enhanced *de novo* shoot regeneration capability (Li et al., 2011). In this study, we found additional targets of MET1-dependent CG methylation. The CG-methylated and MET1-down-regulated genes were enriched for light and cytokinin signaling. In particular, *CRY1*, which is CG-methylated by MET1, was linked to cytokinin signaling genes, as suggested previously (Gangappa and Botto, 2016; Vandenbussche et al., 2007), although detailed molecular connections need to be elucidated.

Each step of the plant regeneration process requires a balance between auxin and cytokinin signaling. A high auxin-to-cytokinin ratio promotes callus formation (Atta et al., 2009; Skoog and Miller, 1957; Sugimoto et al., 2010), whereas a low auxin-to-cytokinin ratio promotes *de novo* shoot regeneration (Skoog and Miller, 1957). MET1-dependent CG methylation suppresses the blue light receptor gene *CRY1*, and subsequently inhibits cytokinin signaling and shoot identity establishment in calli. The *met1-3* mutant displayed higher expression of *CRY1* and consequently that of cytokinin signaling genes. Consistently, shoot regeneration was reduced in the *cry1-1* mutant, possibly because of attenuated cytokinin signaling, but increased in the *met1-3* mutant. Overall, our data suggest that MET1 catalyzes CG methylation and silences light signaling, in part, via the repression of *CRY1*. Light signaling exhibits extensive crosstalk with hormone signaling pathways, especially cytokinin signaling. In *met1-3*, enhanced light and cytokinin signaling promotes shoot identity establishment and *de novo* shoot organogenesis.

Note: Supplementary information is available on the Molecules and Cells website (www.molcells.org).

ACKNOWLEDGMENTS

This work was supported by the Basic Science Research (NRF-2019R1I1A1A01061376 to S.S.; NRF-2019R1A2C2006915 to P.J.S.) and Basic Research Laboratory (NRF-2020R1A4A2002901 to P.J.S.) programs provided by the National Research Foundation of Korea, by the National Research Foundation of Korea, and by the Creative-Pioneering Researchers Program through Seoul National University (0409-20200281 to P.J.S.).

AUTHOR CONTRIBUTIONS

P.J.S. conceived the project. S.S. conducted bioinformatics analyses. H.G.L. performed experiments. S.S. wrote the first draft of manuscript. P.J.S. revised the manuscript. All authors read and approved the final manuscript.

CONFLICT OF INTEREST

The authors have no potential conflicts of interest to disclose.

ORCID

Sangrea Shim https://orcid.org/0000-0002-2439-0803
Pil Joon Seo https://orcid.org/0000-0002-5499-3138

REFERENCES

Atta, R., Laurens, L., Boucheron-Dubuisson, E., Guivarc'h, A., Carnero, E., Giraudat-Pautot, V., Rech, P., and Chriqui, D. (2009). Pluripotency of Arabidopsis xylem pericycle underlies shoot regeneration from root and hypocotyl explants grown *in vitro*. Plant J. *57*, 626-644.

Bartee, L., Malagnac, F., and Bender, J. (2001). *Arabidopsis cmt3* chromomethylase mutations block non-CG methylation and silencing of an endogenous gene. Genes Dev. *15*, 1753-1758.

Baubec, T., Ivánek, R., Lienert, F., and Schübeler, D. (2013). Methylation-dependent and -independent genomic targeting principles of the MBD protein family. Cell *153*, 480-492.

Bhatia, H., Khemka, N., Jain, M., and Garg, R. (2018). Genome-wide bisulphite-sequencing reveals organ-specific methylation patterns in chickpea. Sci. Rep. *8*, 9704.

Brackertz, M., Boeke, J., Zhang, R., and Renkawitz, R. (2002). Two highly related p66 proteins comprise a new family of potent transcriptional repressors interacting with MBD2 and MBD3. J. Biol. Chem. *277*, 40958-40966.

Cao, X. and Jacobsen, S.E. (2002a). Role of the *Arabidopsis DRM* methyltransferases in de novo DNA methylation and gene silencing. Curr. Biol. *12*, 1138-1144.

Cao, X. and Jacobsen, S.E. (2002b). Locus-specific control of asymmetric and CpNpG methylation by the *DRM* and *CMT3* methyltransferase genes. Proc. Natl. Acad. Sci. U. S. A. *99*(Suppl 4), 16491-16498.

Chen, M., Ha, M., Lackey, E., Wang, J., and Chen, Z.J. (2008). RNAi of *met1* reduces DNA methylation and induces genome-specific changes in gene expression and centromeric small RNA accumulation in Arabidopsis allopolyploids. Genetics *178*, 1845-1858.

Chen, X., Schönberger, B., Menz, J., and Ludewig, U. (2018). Plasticity of DNA methylation and gene expression under zinc deficiency in Arabidopsis roots. Plant Cell Physiol. *59*, 1790-1802.

Dubrovsky, J.G., Doerner, P.W., Colón-Carmona, A., and Rost, T.L. (2000). Pericycle cell proliferation and lateral root initiation in Arabidopsis. Plant Physiol. *124*, 1648-1657.

Fan, M., Xu, C., Xu, K., and Hu, Y. (2012). LATERAL ORGAN BOUNDARIES DOMAIN transcription factors direct callus formation in *Arabidopsis* regeneration. Cell Res. *22*, 1169-1180.

Feng, Z., Zhu, J., Du, X., and Cui, X. (2012). Effects of three auxin-inducible LBD members on lateral root formation in *Arabidopsis thaliana*. Planta *236*, 1227-1237.

Fujita, N., Watanabe, S., Ichimura, T., Ohkuma, Y., Chiba, T., Saya, H., and Nakao, M. (2003). MCAF mediates MBD1-dependent transcriptional repression. Mol. Cell. Biol. *23*, 2834-2843.

Fukushige, S., Kondo, E., Gu, Z., Suzuki, H., and Horii, A. (2006). RET finger protein enhances MBD2- and MBD4-dependent transcriptional repression. Biochem. Biophys. Res. Commun. *351*, 85-92.

Gaillochet, C. and Lohmann, J.U. (2015). The never-ending story: from pluripotency to plant developmental plasticity. Development *142*, 2237-2249.

Gangappa, S.N. and Botto, J.F. (2016). The multifaceted roles of HY5 in plant growth and development. Mol. Plant *9*, 1353-1365.

Gaspar, J.M. and Hart, R.P. (2017). DMRfinder: efficiently identifying differentially methylated regions from MethylC-seq data. BMC Bioinformatics *18*, 528.

Harris, C.J., Scheibe, M., Wongpalee, S.P., Liu, W., Cornett, E.M., Vaughan, R.M., Li, X., Chen, W., Xue, Y., Zhong, Z., et al. (2018). A DNA methylation reader complex that enhances gene transcription. Science *362*, 1182-1186.

He, C., Chen, X., Huang, H., and Xu, L. (2012). Reprogramming of H3K27me3 is critical for acquisition of pluripotency from cultured *Arabidopsis* tissues. PLoS Genet. *8*, e1002911.

Ikeuchi, M., Ogawa, Y., Iwase, A., and Sugimoto, K. (2016). Plant regeneration: cellular origins and molecular mechanisms. Development *143*, 1442-1451.

Ingouff, M., Selles, B., Michaud, C., Vu, T.M., Berger, F., Schorn, A.J., Autran, D., Van Durme, M., Nowack, M.K., Martienssen, R.A., et al. (2017). Live-cell analysis of DNA methylation during sexual reproduction in *Arabidopsis* reveals context and sex-specific dynamics controlled by noncanonical RdDM. Genes Dev. *31*, 72-83.

Ishihara, H., Sugimoto, K., Tarr, P.T., Temman, H., Kadokura, S., Inui, Y., Sakamoto, T., Sasaki, T., Aida, M., Suzuki, T., et al. (2019). Primed histone demethylation regulates shoot regenerative competency. Nat. Commun. *10*, 1786.

Ito, T., Nishio, H., Tarutani, Y., Emura, N., Honjo, M.N., Toyoda, A., Fujiyama, A., Kakutani, T., and Kudoh, H. (2019). Seasonal stability and dynamics of DNA methylation in plants in a natural environment. Genes *10*, 544.

Jeddeloh, J.A., Bender, J., and Richards, E.J. (1998). The DNA methylation locus *DDM1* is required for maintenance of gene silencing in *Arabidopsis*. Genes Dev. *12*, 1714-1725.

Johnson, L.M., Bostick, M., Zhang, X., Kraft, E., Henderson, I., Callis, J., and Jacobsen, S.E. (2007). The SRA methyl-cytosine-binding domain links DNA and histone methylation. Curr. Biol. *17*, 379-384.

Kareem, A., Durgaprasad, K., Sugimoto, K., Du, Y., Pulianmackal, A.J., Trivedi, Z.B., Abhayadev, P.V., Pinon, V., Meyerowitz, E.M., Scheres, B., et al. (2015). *PLETHORA* genes control regeneration by a two-step mechanism. Curr. Biol. *25*, 1017-1030.

Kim, J., Yang, W., Forner, J., Lohmann, J.U., Noh, B., and Noh, Y. (2018). Epigenetic reprogramming by histone acetyltransferase HAG1/AtGCN5 is required for pluripotency acquisition in *Arabidopsis*. EMBO J. *37*, e98726.

Kim, M.J., Lee, H.J., Choi, M.Y., Kang, S.S., Kim, Y.S., Shin, J.K., and Choi, W.S. (2021). UHRF1 induces methylation of the *TXNIP* promoter and down-regulates gene expression in cervical cancer. Mol. Cells *44*, 146-159.

Koornneef, M., Hanhart, C.J., and van der Veen, J.H. (1991). A genetic and physiological analysis of late flowering mutants in *Arabidopsis thaliana*. Mol. Gen. Genet. *229*, 57-66.

Koornneef, M., Rolff, E., and Spruit, C.J.P. (1980). Genetic control of light-inhibited hypocotyl elongation in *Arabidopsis thaliana* (L.) Heynh. Z. Pflanzenphysiol. *100*, 147-160.

Krueger, F. and Andrews, S.R. (2011). Bismark: a flexible aligner and methylation caller for Bisulfite-Seq applications. Bioinformatics *27*, 1571-1572.

Lang, Z., Wang, Y., Tang, K., Tang, D., Datsenka, T., Cheng, J., Zhang, Y., Handa, A.K., and Zhu, J.K. (2017). Critical roles of DNA demethylation in the activation of ripening-induced genes and inhibition of ripening-repressed genes in tomato fruit. Proc. Natl. Acad. Sci. U. S. A. *114*, E4511-E4519.

Langmead, B. and Salzberg, S.L. (2012). Fast gapped-read alignment with Bowtie 2. Nat. Methods *9*, 357-359.

Lee, K., Park, O.S., and Seo, P.J. (2016). RNA-seq analysis of the *Arabidopsis* transcriptome in pluripotent calli. Mol. Cells *39*, 484-494.

Lee, K., Park, O.S., and Seo, P.J. (2017). *Arabidopsis* ATXR2 deposits H3K36me3 at the promoters of *LBD* genes to facilitate cellular dedifferentiation. Sci. Signal. *10*, eaan0316.

Lee, K. and Seo, P.J. (2018). Dynamic epigenetic changes during plant regeneration. Trends Plant Sci. *23*, 235-247.

Li, W., Liu, H., Cheng, Z.J., Su, Y.H., Han, H.N., Zhang, Y., and Zhang, X.S. (2011). DNA methylation and histone modifications regulate *de novo* shoot regeneration in *Arabidopsis* by modulating *WUSCHEL* expression and auxin signaling. PLoS Genet. *7*, e1002243.

Liang, L., Chang, Y., Lu, J., Wu, X., Liu, Q., Zhang, W., Su, X., and Zhang, B. (2019). Global methylomic and transcriptomic analyses reveal the broad participation of DNA methylation in daily gene expression regulation of *Populus trichocarpa*. Front. Plant Sci. *10*, 243.

Lin, C., Yang, H., Guo, H., Mockler, T., Chen, J., and Cashmore, A.R. (1998). Enhancement of blue-light sensitivity of Arabidopsis seedlings by a blue light receptor cryptochrome 2. Proc. Natl. Acad. Sci. U. S. A. *95*, 2686-2690.

Lindroth, A.M., Cao, X., Jackson, J.P., Zilberman, D., McCallum, C.M., Henikoff, S., and Jacobsen, S.E. (2001). Requirement of *CHROMOMETHYLASE3* for maintenance of CpXpG methylation. Science *292*, 2077-2080.

Liu, H., Zhang, H., Dong, Y.X., Hao, Y.J., and Zhang, X.S. (2018). *DNA METHYLTRANSFERASE1*-mediated shoot regeneration is regulated by cytokinin-induced cell cycle in *Arabidopsis*. New Phytol. *217*, 219-232.

Liu, J., Sheng, L., Xu, Y., Li, J., Yang, Z., Huang, H., and Xu, L. (2014). *WOX11* and *12* are involved in the first-step cell fate transition during de novo root organogenesis in *Arabidopsis*. Plant Cell *26*, 1081-1093.

Liu, Z.W., Zhou, J.X., Huang, H.W., Li, Y.Q., Shao, C.R., Li, L., Cai, T., Chen, S., and He, X.J. (2016). Two components of the RNA-directed DNA methylation pathway associate with MORC6 and silence loci targeted by MORC6 in *Arabidopsis*. PLoS Genet. *12*, e1006026.

Meng, W.J., Cheng, Z.J., Sang, Y.L., Zhang, M.M., Rong, X.F., Wang, Z.W., Tang, Y.Y., and Zhang, X.S. (2017). Type-B ARABIDOPSIS RESPONSE REGULATORs specify the shoot stem cell niche by dual regulation of *WUSCHEL*. Plant Cell *29*, 1357-1372.

Nameth, B., Dinka, S.J., Chatfield, S.P., Morris, A., English, J., Lewis, D., Oro, R., and Raizada, M.N. (2013). The shoot regeneration capacity of excised Arabidopsis cotyledons is established during the initial hours after injury and is modulated by a complex genetic network of light signalling. Plant Cell Environ. *36*, 68-86.

Obayashi, T., Aoki, Y., Tadaka, S., Kagaya, Y., and Kinoshita, K. (2018). ATTED-II in 2018: a plant coexpression database based on investigation of the statistical property of the mutual rank index. Plant Cell Physiol. *59*, e3.

Ortega-Galisteo, A.P., Morales-Ruiz, T., Ariza, R.R., and Roldán-Arjona, T. (2008). Arabidopsis DEMETER-LIKE proteins DML2 and DML3 are required for appropriate distribution of DNA methylation marks. Plant Mol. Biol. *67*, 671-681.

Penterman, J., Zilberman, D., Huh, J.H., Ballinger, T., Henikoff, S., and Fischer, R.L. (2007). DNA demethylation in the *Arabidopsis* genome. Proc. Natl. Acad. Sci. U. S. A. *104*, 6752-6757.

Quinlan, A.R. and Hall, I.M. (2010). BEDTools: a flexible suite of utilities for comparing genomic features. Bioinformatics *26*, 841-842.

Ramírez, F., Dündar, F., Diehl, S., Grüning, B.A., and Manke, T. (2014). deepTools: a flexible platform for exploring deep-sequencing data. Nucleic Acids Res. *42*(Web Server issue), W187-W191.

Saze, H., Scheid, O., and Paszkowski, J. (2003). Maintenance of CpG methylation is essential for epigenetic inheritance during plant gametogenesis. Nat. Genet. *34*, 65-69.

Shim, S., Lee, H.G., Park, O.S., Shin, H., Lee, K., Lee, H., Huh, J.H., and Seo, P.J. (2021). Dynamic changes in DNA methylation occur in TE regions and affect cell proliferation during leaf-to-callus transition in Arabidopsis. Epigenetics 2021 Jan 15 [Epub]. https://doi.org/10.1080/15592294.2021.1872927

Skoog, F. and Miller, C.O. (1957). Chemical regulation of growth and organ formation in plant tissues cultured in vitro. Symp. Soc. Exp. Biol. *11*, 118-130.

Smallwood, S.A., Lee, H.J., Angermueller, C., Krueger, F., Saadeh, H., Peat, J., Andrews, S.R., Stegle, O., Reik, W., and Kelsey, G. (2014). Single-cell genome-wide bisulfite sequencing for assessing epigenetic heterogeneity. Nat. Methods *11*, 817-820.

Stassen, J.H.M., López, A., Jain, R., Pascual-Pardo, D., Luna, E., Smith, L.M., and Ton, J. (2018). The relationship between transgenerational acquired resistance and global DNA methylation in Arabidopsis. Sci. Rep. *8*, 14761.

Sugimoto, K., Jiao, Y., and Meyerowitz, E.M. (2010). *Arabidopsis* regeneration from multiple tissues occurs via a root development pathway. Dev. Cell *18*, 463-471.

Usadel, B., Poree, F., Nagel, A., Lohse, M., Czedik-Eysenberg, A., and Stitt, M. (2009). A guide to using MapMan to visualize and compare Omics data in plants: a case study in the crop species, Maize. Plant Cell Environ. *32*, 1211-1129.

Vandenbussche, F., Habricot, Y., Condiff, A.S., Maldiney, R., Straeten, D.V.D., and Ahmad, M. (2007). HY5 is a point of convergence between cryptochrome and cytokinin signalling pathways in *Arabidopsis thaliana*. Plant J. *49*, 428-441.

Waterfield, M., Khan, I.S., Cortez, J.T., Fan, U., Metzger, T., Greer, A.,

Fasano, K., Martinez-Llordella, M., Pollack, J.L., Erle, D.J., et al. (2014). The transcriptional regulator Aire co-opts the repressive ATF7ip-MBD1 complex for induction of immune tolerance. Nat. Immunol. *15*, 258-265.

Yoo, H., Park, K., Lee, J., Lee, S., and Choi, Y. (2021). An optimized method for the construction of a DNA methylome from small quantities of tissue or purified DNA from *Arabidopsis* embryo. Mol. Cells *44*, 602-612.

Yu, X., Liu, H., Klejnot, J., and Lin, C. (2010). The cryptochrome blue light receptors. Arabidopsis Book *8*, e0135.

Zemach, A. and Grafi, G. (2003). Characterization of *Arabidopsis thaliana* methyl-CpG-binding domain (MBD) proteins. Plant J. *34*, 565-572.

Zhang, T.Q., Lian, H., Zhou, C.M., Xu, L., Jiao, Y., and Wang, J.W. (2017). A two-step model for de novo activation of *WUSCHEL* during plant shoot regeneration. Plant Cell *29*, 1073-1087.

Zhou, M., Sng, N.J., LeFrois, C.E., Paul, A.L., and Ferl, R.J. (2019). Epigenomics in an extraterrestrial environment: organ-specific alteration of DNA methylation and gene expression elicited by spaceflight in *Arabidopsis thaliana*. BMC Genomics *20*, 205.

Zilberman, D., Gehring, M., Tran, R.K., Ballinger, T., and Henikoff, S. (2007). Genome-wide analysis of *Arabidopsis thaliana* DNA methylation uncovers an interdependence between methylation and transcription. Nat. Genet. *39*, 61-69.

Zubko, E., Gentry, M., Kunova, A., and Meyer, P. (2012). *De novo* DNA methylation activity of METHYLTRANSFERASE 1 (MET1) partially restores body methylation in *Arabidopsis thaliana*. Plant J. *71*, 1029-1037.